American Journal of Nano Research and Applications
2018; 6(3): 60-66
http://www.sciencepublishinggroup.com/j/nano
doi: 10.11648/j.nano.20180603.11
ISSN: 2575-3754 (Print); ISSN: 2575-3738 (Online)

The Crystallization Kinetics, Structural and Magnetic Properties of $Fe_{72.5}Ag_2Nb_3Si_{13.5}B_9$ Amorphous Ribbons as Affected by Annealing

Mohammad Mahmuduzzaman Tawhid[1], Sujit Kumer Shil[1, *], Mohammad Tahmid Shihab[1], Shibendra Shekher Sikder[1], Mohammad Abdul Gafur[2]

[1]Department of Physics, Khulna University of Engineering and Technology, Khulna, Bangladesh

[2]Bangladesh Council of Scientific and Industrial Research, Dhaka, Bangladesh

Email address:

sujitphy.kuet@gmail.com (S. K. Shil)

[*]Corresponding author

To cite this article:

Md. Mahmuduzzaman Tawhid, Sujit Kumer Shil, Md. Tahmid Shihab, Shibendra Shekher Sikder, Md. Abdul Gafur. The Crystallization Kinetics, Structural and Magnetic Properties of $Fe_{72.5}Ag_2Nb_3Si_{13.5}B_9$ Amorphous Ribbons as Affected by Annealing. *American Journal of Nano Research and Applications*. Vol. 6, No. 3, 2018, pp. 60-66. doi: 10.11648/j.nano.20180603.11

Received: August 3, 2018; **Accepted**: September 15, 2018; **Published**: October 22, 2018

Abstract: The amorphous ribbon of composition $Fe_{72.5}Ag_2Nb_3Si_{13.5}B_9$ has been prepared by rapid solidification technique under an atmosphere of pure argon and the amorphous nature has been confirmed by X-ray diffraction (XRD). The crystallization behavior and the nanocrystal formation have been studied by Differential Thermal Analysis (DTA) and XRD. The effect of annealing has been explained on the basis of XRD spectra. Magnetization measurements have been carried out using vibrating sample magnetometer (VSM). The activation energy for crystallization is evaluated by Kissinger's plot. The peak temperature is found to be shifted towards the higher value with heating rate. The peak shift indicates the change of the values of Si-content of nanograins and therefore, the change of the lattice parameter of nanograins. At higher annealing temperature (T_a) the crystallization peak becomes smaller and displays diffused character meaning that substantial amount of crystallization of α-Fe (Si) phase has already been completed. The activation energy for α-Fe-(Si) phase is found to be 5.78 eV and 0.164 eV for before and after annealing respectively. The saturation magnetization (M_s) and Curie temperature (T_c) were found 114 emu/g and 305°C respectively. The sharp fall of magnetization at T_c is obtained which is an indication of homogeneity of the material.

Keywords: DTA, Annealing Temperature, Grain Size, Saturation Magnetization, Curie Temperature

1. Introduction

It has been well established by the time through extensive research that the addition of Cu and Nb, simultaneously with Fe-Si-B based amorphous alloys is the necessary condition for the extraordinary soft magnetic properties called FINEMET having composition $Fe_{73.5}Nb_3Cu_1Si_{13.5}B_9$, developed in 1988 by Yoshizawa, Oguma and Yamauchi at Hitachi Metals Ltd. [1]. The Cu additives play a key role in the formation of the nucleation centres and Nb inhibits the grain growth [2]. This addition extends the temperature range between the primary crystallization of α-Fe(Si) phase and secondary crystallization of Fe_2B phase for achieving superior magnetic properties [3]. It should be stressed again that good soft magnetic properties require not only a small grain size but at the same time the absence of boron compounds. The separation between the primary crystallization of bcc α-Fe(Si) and the precipitation of Fe_2B compounds is not only determined by Cu and Nb addition but also decrease with increasing content. This put a further constraint on the alloy composition namely that boron content should be kept at a low or moderate level in order to obtain an optimum nanoscaled structure. Amorphous alloys provide an extremely convenient precursor material for

preparation of nanocrystals through the crystallization process controlled by thermal treatments [4-7]. Müller *et. al.* [8] studied the influence of Cu/ Nb content and annealing condition on the microstructure and the magnetic properties of FINEMET alloys. Grain size, phase composition and transition temperature were observed, depend on the Cu/ Nb content. These represent a new family of excellent soft magnetic core materials and have stimulated an enormous research activity due to their potential applications [9–12]. Investigations have been carried out on the effect of substitution of Au for Cu in the FINEMET on the crystallization behavior and magnetic properties [13]. It has been found that Au behaves similarly as Cu on crystallization behavior and magnetic properties. This paper focuses on the experimental investigation of crystallization behavior, nanocrystalline structure formation and magnetic properties of $Fe_{72.5}Ag_2Nb_3Si_{13.5}B_9$ alloys in the amorphous and annealed states.

2. Materials and Methods

The amorphous ribbon of composition $Fe_{72.5}Ag_2Nb_3Si_{13.5}B_9$ was prepared from high purity Fe (99.9 %), Ag (99.9%), Nb (99.9 %), Si (99.9 %) and B (99.9 %). The ribbons were produced in an arc furnace on a water-cooled copper hearth by a single roller melt-spinning technique under an atmosphere of pure argon at the Centre of Materials Science, National University of Hanoi, Vietnam. The wheel velocity was about 34 m/s. The ribbons were annealed in a vacuum heat treatment furnace at 550, 600, 650, 700 and 750°C respectively for constant time 30 minutes and then cooled down to the room temperature. Crystallization phase analysis was carried out by DTA. The activation energy for crystallization of primary and secondary phases have been calculated using Kissinger's equation [14]: $E = -kT_p \ln\left(\frac{\beta}{T_p^2}\right)$, where β is the heating rate, T_p is the crystallization peak temperature, E is the activation energy and k is the Boltzman's constant. Amorphousity of the ribbon and nanocrystalline structure have been observed by XRD (Philips X 'Pert PRO XRD) with Cu-Kα radiation. Lattice parameter (a_0) were calculated using equations $2d\sin\theta = \lambda$ and $a_0 = d\sqrt{2}$, where λ=1.54178 Å for $Cu-K_\alpha$ radiation. Grain size (D_g) of all annealed samples of the alloy composition has been determined using Scherrer method. Si contents were calculated using the equation: $X = \frac{(a_0 - 2.8812)}{0.0022}$, where X is at.% Si in the nanograins. Magnetic properties such as field dependent specific magnetization and temperature dependent magnetization were performed by using VSM.

3. Results and Discussion

3.1. DTA

DTA traces of as-cast amorphous ribbons $Fe_{72.5}Ag_2Nb_3Si_{13.5}B_9$ with heating at the rate of 10–60°C/min at the step of 10°C with continuous heating from room temperature to 800°C are shown in the figure 1. It is clear from Figure 1(a) to 1(f) that one exothermic peak is found. The soft magnetic properties correspond to the primary crystallization of α-Fe-(Si) phase initiated at T_{x_1}. The peak temperature, T_{P_1} displays exothermic peak, i.e., release of heat during the crystallization of α-Fe-(Si) phase. It is observed that the crystallization of the phase has occurred over a wide range of temperatures. It is also observed that the peak temperature shifted towards the higher value and the crystallization temperature range increases with the increase of heating rate. That means it requires more heat energy for the formation of crystalline phase with increasing heating rate. The heat consumption is observed during the primary crystallization. The peak is shifting in the range from 579°C-607°C is evident from the figure1. From the Figure 2(a) and Fig. 2(b) the activation energy for the α-Fe-(Si) phase is found to be 5.78 eV and 0.164 eV for before and after annealing respectively. The values of crystallization onset temperature, peak temperature with respect to heating rate and activation energy are listed in the Table 1.

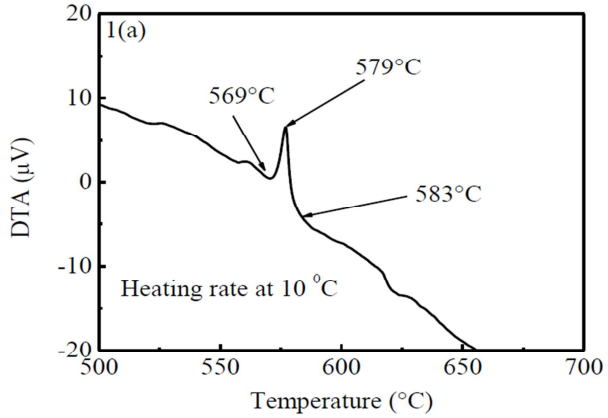

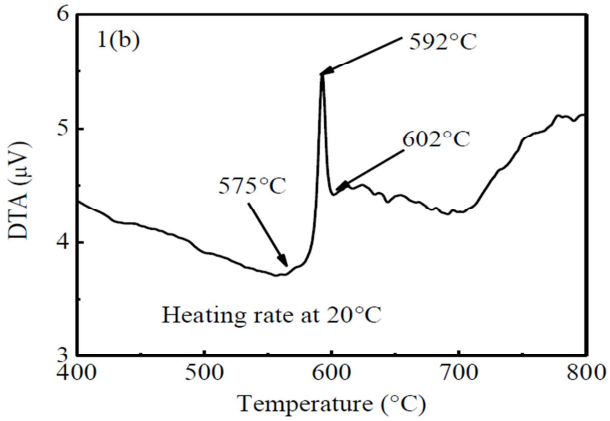

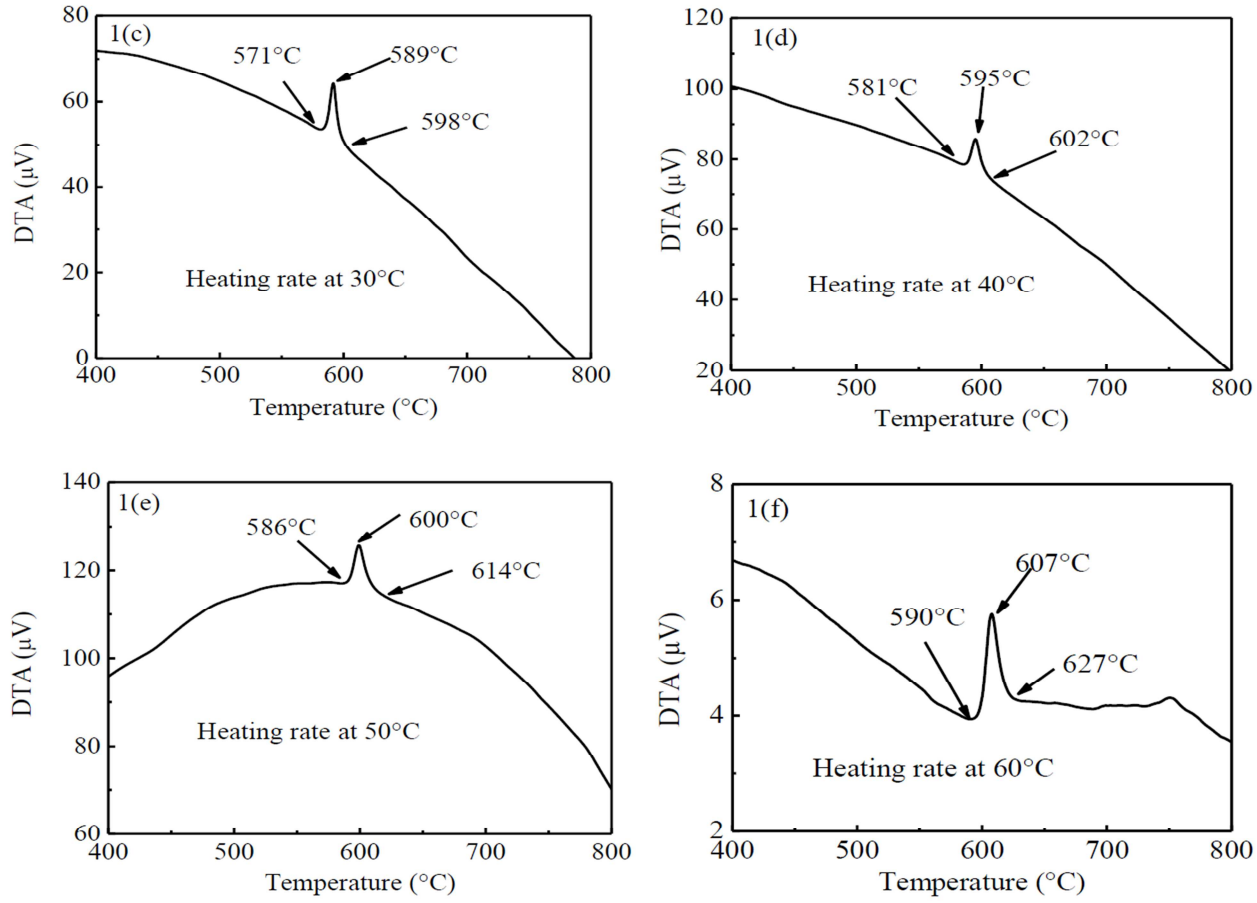

Figure 1. *DTA trace of as cast amorphous ribbon $Fe_{72.5}Ag_2Nb_3Si_{13.5}B_9$ at the heating rate of (a)10°C/min (b) 20°C/min (c) 30°C/min (d) 40°C/min (e) 50°C/min (f) 60°C/min.*

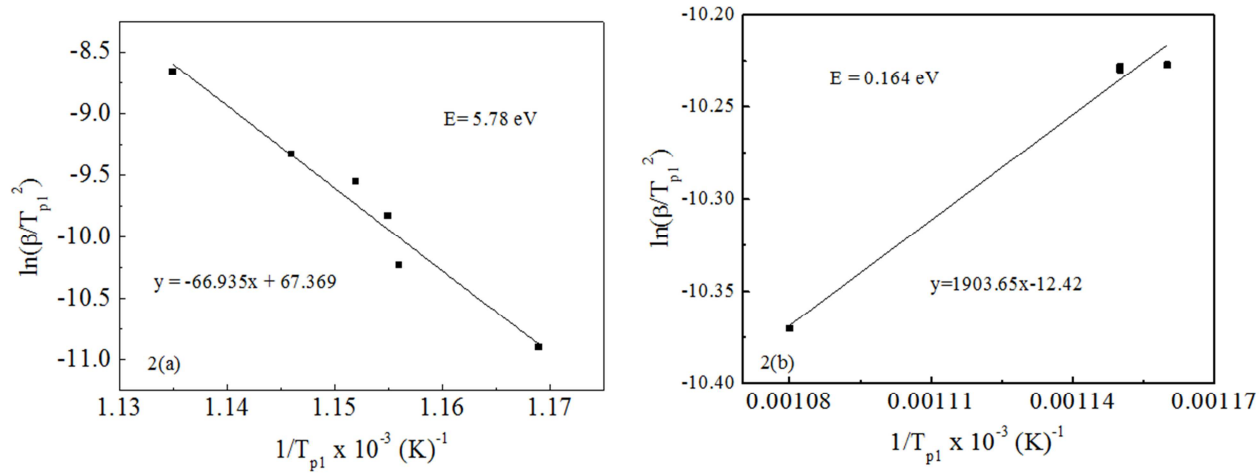

Figure 2. *Kissinger's plot to determine the activation energy of α-Fe-(Si) phase for (a) before annealing (b) after annealing.*

The DTA traces of $Fe_{72.5}Ag_2Nb_3Si_{13.5}B_9$ alloy in the as cast state and annealed at different temperatures for 2 hours are shown in Figure 3(a) to 3(d) respectively. It is observed from the DTA scan that the onset temperature for the sample $Fe_{72.5}Ag_2Nb_3Si_{13.5}B_9$ annealed at 550°C is almost unchanged with respect to its amorphous precursor which is quite logical since 550°C is still lower than T_{x_1} = 579°C. But the same sample when annealed at T_a = 600°C and 650°C which are higher than the onset of crystallization temperature of T_{x_1} = 579°C, the crystallization peak is becoming smaller and display diffused character meaning that substantial amount of crystallization, $\alpha - Fe(Si)$ phase has already been completed when annealed at 600°C and 650°C for 2 hours.

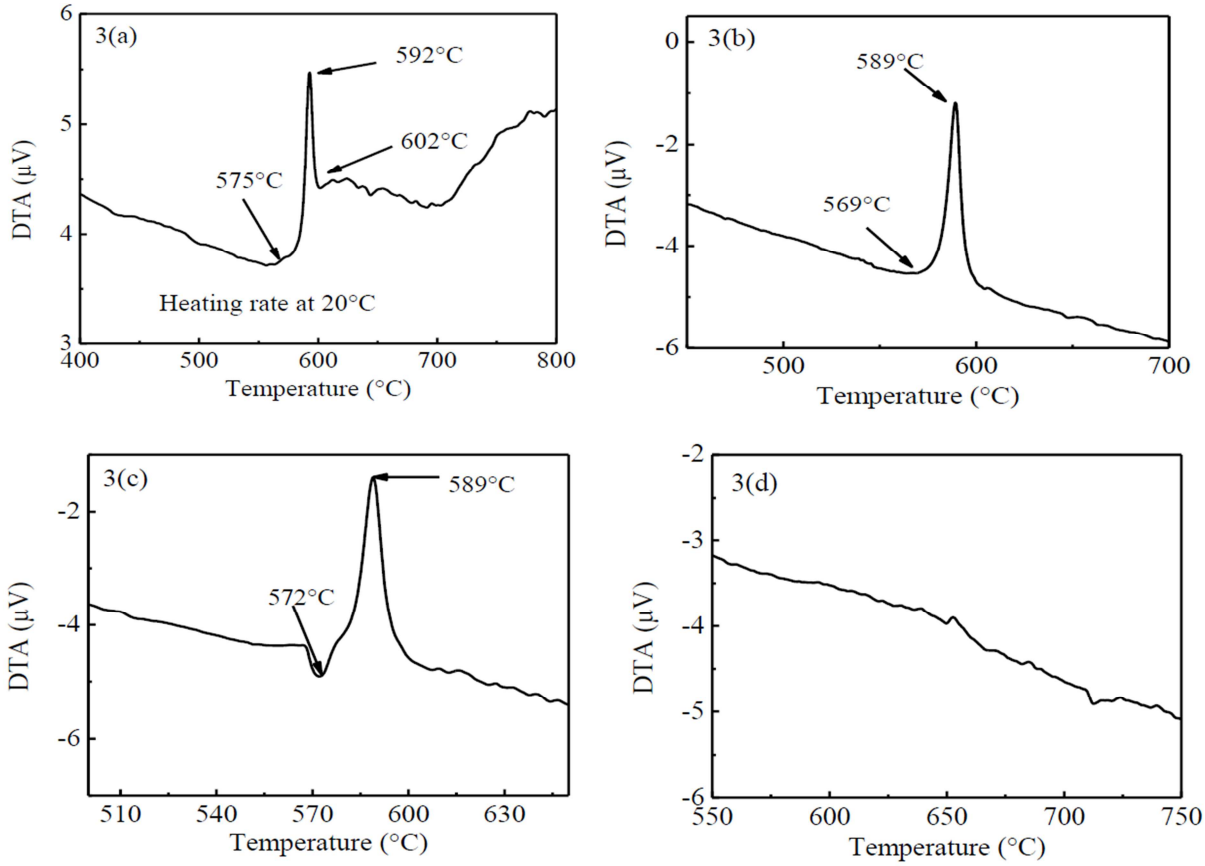

Figure 3. *DTA traces of nanocrystalline amorphous ribbon with composition $Fe_{72.5}Ag_2Nb_3Si_{13.5}B_9$ at the heating rate of 20° C/min for (a) as cast and annealed at (b) 550°C (c) 600°C (d) 650°C.*

Table 1. *The values of crystallization onset temperature, peak temperature with respect to heating rate and activation energy of the nanocrystalline amorphous ribbon with composition $Fe_{72.5}Ag_2Nb_3Si_{13.5}B_9$.*

Heating rate β (°C/min)	Onset temperature T_x (°C)	Peak temperature T_p (°C)	Temperature range of the state (°C)	Activation energy of the peak before annealing (eV)	Activation energy of the peak after annealing (eV)
10	569	579	10		
20	575	592	17		
30	571	598	27	5.78	0.164
40	581	595	14		
50	586	600	14		
60	590	607	17		

3.2. XRD

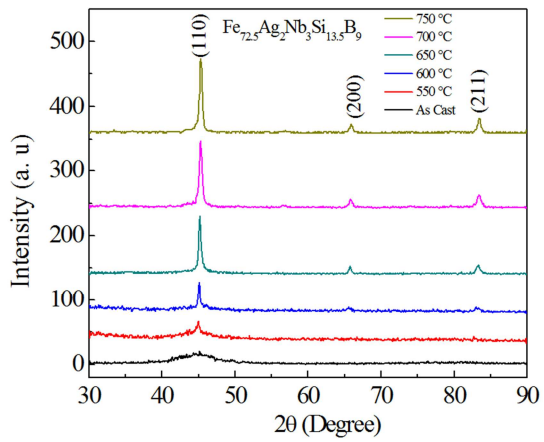

Figure 4. *XRD spectra of $Fe_{72.5}Ag_2Nb_3Si_{13.5}B_9$ alloys of as cast and annealed at different temperatures for constant annealing time 2 hours.*

The XRD spectra of as cast and sample annealed from 550 to 750°C have been presented in the figure 4. In the case of as cast state, there has a broadened peak which could be the evidence of amorphous nature. When the sample annealed at 550°C, it exhibited small peak around $2\theta = 45^\circ$ at the position of d_{110} reflection which is generally known as diffuse hallow. This diffuse hallow indicates the amorphous nature of the sample. It means at this temperature, no crystallization peak has been detected. With the increasing of T_a, (110) peak becomes sharper which means the grains are growing bigger. The value of full width half maxima (FWHM) of the peak annealed at 550°C was not detected due to the lack of sharp peak. For the higher T_a, the FWHM value is getting smaller. It shows that the crystallization occurs to a good extent at the higher T_a. The crystallization onset temperatures from DTA experiment for different heating rates were found in the range of 569 to 590°C, which shows a good consistency with the

XRD results. The lattice parameter, the silicon content in bcc nanograins and grain size of α-Fe(Si) grain can easily be calculated from the fundamental peak of (110) reflections. All results are shown in Table 2.

Figure 5 presents the inverse relationship between lattice parameter and silicon content with T_a. At higher T_a, with increasing T_a, Si-content is observed to rise, explained by the fact that at higher temperatures silicon diffuses out of nanograins due to crystallization which is consistent with the result of other FINEMET's [15]. Si having a smaller atomic size compared to Fe, diffuses in the α-Fe(Si) lattice during annealing at different temperatures which results in a contraction of α-Fe(Si) lattice. So the more diffusion of Si, there should be more contraction of the α-Fe(Si) lattice and thereby, the decrease of a_0. However the decrease in lattice parameter is evident at higher annealing temperature when the diffusion of Si became easier at that temperature due to stress-relief in microstructure caused by heat treatment.

Figure 6 shows the change of grain size (D_g) with T_a. The increase of T_a initiates partitioning α-Fe(Si) phase and thus grain growth due to formation of nanocrystalline α-Fe(Si) grains. In the range of T_a from 600°C to 750°C, the D_g remains in the range of 50 to 69 nm corresponding to soft magnetic α-Fe(Si) phases. The grain size increasing with increasing T_a up to 650°C but with further increasing T_a, the D_g increases which may be resulted due to higher physical distortion and internal strain. These facts reveal that heat treatment temperature should be limited with in 600°C as D_g remains 50 nm to obtain optimum soft magnetic behavior.

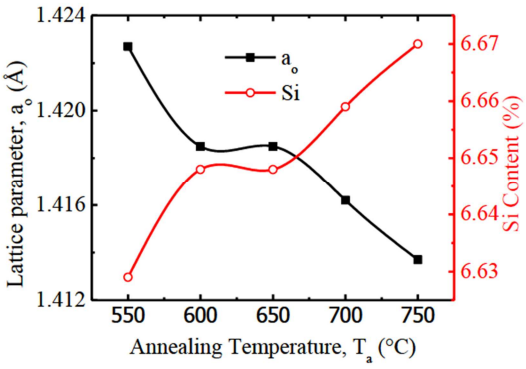

Figure 5. *Change of Si (at. %) content and Lattice Parameter with annealing temperature for the sample with composition* $Fe_{72.5}Ag_2Nb_3Si_{13.5}B_9$.

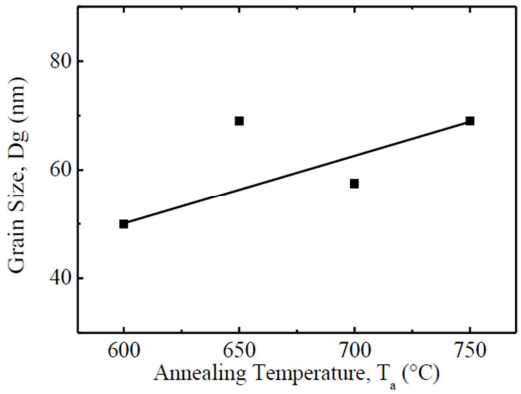

Figure 6. *Change of Grain Size with different annealing temperature for the sample with composition* $Fe_{72.5}Ag_2Nb_3Si_{13.5}B_9$.

Table 2. *XRD data of nanocrystalline* $Fe_{72.5}Ag_2Nb_3Si_{13.5}B_9$ *amorphous ribbon at different annealing temperatures.*

Annealing Temp. in °C	θ (deg.)	d (Å)	B FWHM (deg.)	a_0 (Å)	D_g (nm)	Si (at. %)
As Cast	22.61	2.0028	…….	1.4161	…..	6.66
550	22.50	2.0121	…….	1.4227	…..	6.63
600	22.57	2.0061	0.3010	1.4185	50	6.65
650	22.57	2.0061	0.2178	1.4185	69	6.65
700	22.61	2.0028	0.2614	1.4162	58	6.66
750	22.65	1.9994	0.2179	1.4137	69	6.67

3.3. Field Dependence of Magnetization

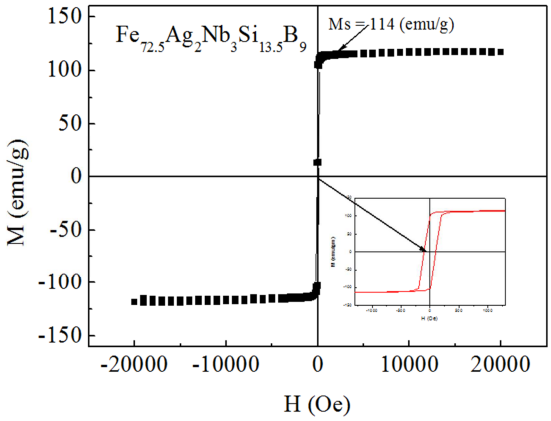

Figure 7. *Magnetization versus magnetic field curves for the alloy with composition* $Fe_{72.5}Ag_2Nb_3Si_{13.5}B_9$.

The magnetization process of the nanocrystalline amorphous ribbon of composition $Fe_{72.5}Ag_2Nb_3Si_{13.5}B_9$ is shown in Figure 7. From the magnetization curve it is clearly evidenced that the M_s is found114 emu/g at room temperature. The small loop area indicates the soft magnetic performance of the ribbon.

3.4. Temperature Dependence of Specific Magnetization

The variation of magnetization (M) as a function of temperature in the range 0°C to 400°C with constant applied field of 10 kOe in the amorphous state for the nanocrystalline amorphous sample with composition $Fe_{72.5}Ag_2Nb_3Si_{13.5}B_9$ is shown in Figure 8.

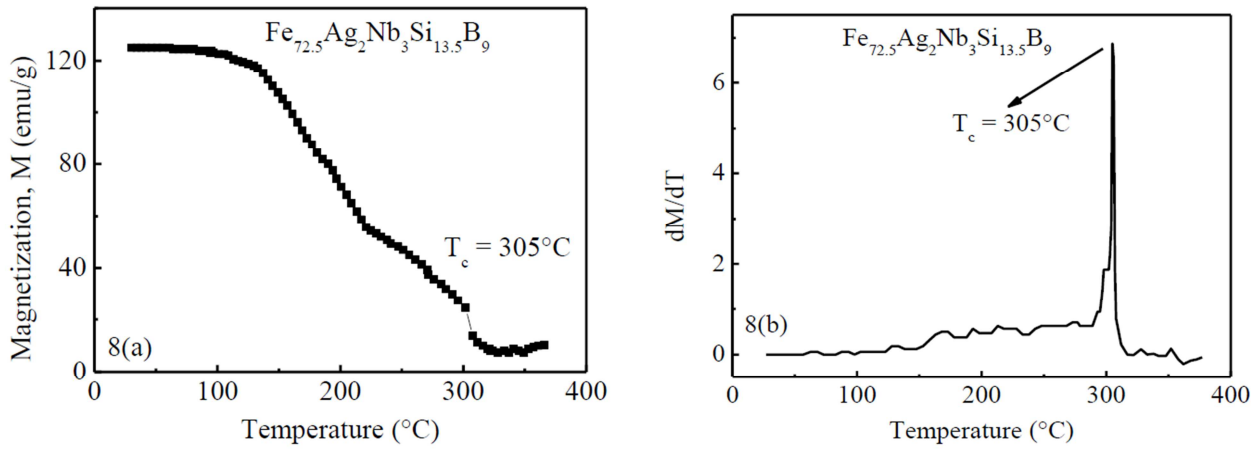

Figure 8. *(a) Temperature dependence of specific magnetization (b)* $\frac{dM}{dT}$ *versus temperature curve of amorphous nanocrystalline ribbon with composition* $Fe_{72.5}Ag_2Nb_3Si_{13.5}B_9$.

It is clearly observed from the curves of Figure 7(a) that the M of the sample decreases gradually with increasing temperature since the thermal energy acts on opposition to the magnetic coupling or exchange energy between neighboring atoms. It is also noticed that as the temperature approaches to the T_c magnetization falls more rapidly near to zero as the thermal energy exceeds the magnetic ordering or the exchange energy. The sharp fall of M at T_c indicates that the material is quite homogeneous. From the Figure 7(b) the T_c is observed 305°C.

4. Conclusion

From the systematic investigation on the crystallization kinetics, structural and magnetic properties the following conclusions can be outlined:

(i) DTA reveals, one exothermic peak which corresponds to crystallization event of α-Fe(Si) phase. The crystallization temperature is obtained in the range from 579 to 607°C for different heating rates before annealing. The saturation temperature is important for stability of α-Fe (Si) phase while it is necessary for fabrication of higher quality inductors. When the sample annealed at 600°C and 650°C which are higher than the onset of crystallization temperature of 579°C, the crystallization peak is becoming smaller and display diffused character meaning that substantial amount of crystallization of $\alpha - Fe(Si)$ phase has already been completed.

(ii) The activation energy of the crystallization phase α-Fe(Si) before and after annealing is found 5.78 eV and 0.164 eV respectively.

(iii) The amorphous state of the as-cast ribbon has been confirmed by XRD. The evolution of the primary crystallization phase on annealed samples has been confirmed as α-Fe(Si) and their sizes have been found from 50 to 69 nm. These facts reveal that heat treatment temperature should be limited with in 600°C as grain size remains 50 nm to obtain optimum soft magnetic behavior, From XRD experiment, the crystallization onset temperature for the sample is found around 600°C which coincides well with the value obtained from DTA.

(iv) The M_s and T_c of the sample at room temperature is 114 emu/g and 305°C respectively. The sharp fall of $\frac{dM}{dT}$ at T_c indicates that the material is quite homogeneous.

Acknowledgements

We are grateful to Bangladesh Council for Scientific and Industrial Research (BCSIR) for giving experimental facilities and cordial co-operations.

References

[1] Yoshizawa, Y., Oguma, S. and Yamauchi, K. (1988) New Fe-based soft magnetic alloys composed of ultra fine grain structure, J. Appl. Phys., 64, 6044 – 6046.

[2] Jing Zhi, Kai-Yuan He, Li-Zbi Cheng and Yu-Jan Fu (1996) Influence of the elements Si/B on the structure and magnetic properties of Nanocrystalline $(FeCuNb)_{77.5}Si_xB_{22.5-x}$ Alloys, J. Magn. Magn. Mater, 153, 315-319.

[3] Herzer, G. (1997) Nanocrystalline Soft Magnetic Alloys. In: Buchow K. H. J., Ed., Handbook of Magnetic Materials, Elsevier B. V., Amsterdam, 10, 415-462.

[4] Herzer, G. (1990) Grain structure and Magnetism of Nanocrystalline Ferromagnetic, IEEE Trans. Magn., 26, 1397-1402.

[5] Hakim, M. A. and Hoque, S. M. (2004) Effect of Structural Parameters on Soft Magnetic properties of two phase nanocrystalline alloy of $Fe_{73.5}Cu_1Ta_3Si_{13.5}B_9$, J. Magn. Magn. Mater., 284, 395-402.

[6] Sarout Noor, Sikder, S. S., Saha D. K. and Hakim, M. A. (2016) Time and Temperature Dependence of Nanocrystalline and Initial Permeability of Finement alloys, Nuclear Science and Application, 15(1), 9-13.

[7] Mondal, S. P., Kazi Hanium Maria, Sikder, S. S., Shamima Chowdhury, Saha, D. K. and Hakim, M. A. (2012) Influence of Annealing Conditions in Nanocrystalline and Ultra soft Magnetic properties of $Fe_{73.5}Cu_1Nb_3Si_{13.5}B_9$, J. Mater, Sci Technol., 28(1), 21-26.

[8] Müller, M., Matterm, N. and Kuhn, U. (1996) Corelation between magnetic and structural properties of Nanocrystalline soft magnetic alloys, J. Magn. Magn. Mater., 157-158, 209-210.

[9] Hakim, M. A., (2004) Magnetic softening of nanocrystalline FeCuNbSiB alloys on annealing, J. Bangladesh Electronic Society, 4, 40-45.

[10] Hoffmann, B. and Kornmuller, S. (1996) Stress-induced magnetic anisotropy in monocrystalline FeCuNbSiB alloy, J. Magn. Magn. Mater., 152, 91-98.

[11] Sikder, S. S. and Asgar, M. A. (1999) The kinetics of atomic and magnetic ordering of atomic and magnetic ordering of the Co-based amorphous ribbons as affected by Iron substitution, Thermochimica Acta, 326, 119–126.

[12] Asgar, M. A. and Sikder, S. S. (1999) Influence of Glass Forming Materials on Atomic and Magnetic ordering of Fe-based Metallic Glass, Indian J. Phys., 73A(4), 493-502.

[13] Saha, D. K. and Hakim, M. A. (2006) Crystallization Behaviour of $Fe_{73.5}Au_1Nb_3Si_{13.5}B_9$", Bang. J. Acad. Sci., 30(2), 177-187.

[14] Kissenger, H. E. (1956) Variation of Peak Temperature with Heating Rate in Differential Thermal Analysis, J. Res. Nat. Bur. Stand., 57, 217-221.

[15] Ratan Krishna Howlader, Sujit Kumer Shil, Shibendra Shekher Sikder, Dilip Kumer Saha (2017) Effect of Annealing Temperature on the Complex Permeability of $(Fe_{0.95}Co_{0.05})_{73.5}Cu_1Nb_3Si_{13.5}B_9$ Nanocrystalline Amorphous Ribbon, Research & Reviews: Journal of Material Sciences, 5(6), 144-148.